Stability of Supported Organometallic Clusters Probed by a Mass-Sensitive TEM Technique

A. Singhal*

Department of Materials Science & Engineering, University of Illinois, Urbana, Illinois 61801

J. Murray Gibson

Department of Physics and Materials Science & Engineering, University of Illinois, Urbana, Illinois 61801

M. M. J. Treacy

NEC Research Institute Inc., Princeton, New Jersey 08540

P. D. Lane

Department of Chemistry, University of Illinois, Urbana, Illinois 61801

J. R. Shapley

Department of Chemistry, University of Illinois, Urbana, Illinois 61801

Received: December 13, 1995; In Final Form: February 23, 1996[⊗]

Using a refined quantitative TEM technique, we measure the relative mass of individual organometallic rhenium clusters on a graphite support. We observe that whereas 6-Re atom species preserve integrity on precipitation from solution, fragmentation and sintering occur in 7- and 8-Re atoms cluster species. These organometallics are candidates as catalytic materials. The technique is based on high-angle dark-field scanning transmission electron microscope (STEM) imaging. The emphasis in this analysis is on using very high angles of scattering to suppress coherence effects from these clusters and on reliably measuring their relative experimental elastic scattering cross sections.

Introduction

Many of the present day research efforts are directed toward design and fabrication of materials of nanometer and subnanometer dimensions.[1−3] Organometallic clusters are potential sources of ultrasmall bare metal clusters for application in catalysis.[4] These materials, when deposited on a support, can provide controlled, finer size distribution as compared to conventionally made catalysts. For a given chemical reaction even a small charge in cluster size can result in a dramatic variation in reactivity.[5] Therefore, it can be vital to determine the cluster size distribution. We know a lot about these clusters in solution, but it is critical to understand how these clusters behave when deposited on a substrate.[6] The size evolution of these clusters on different supports is of special interest in catalysis.

Most supported catalyst systems have a size distribution and to understand the microscopic origins of activity and sintering, cluster size measurements, e.g., by imaging or spectroscopy, are useful. The surface area of supported metal particles can be readily measured by gas adsorption. Spectroscopic measurements of particle size can be unreliable because of lower scattering cross sections and the difficulties of ingenuous interpretation in such analyses. Microscopy-based techniques have been proposed by Poppa[7] and Treacy.[9] While considerable effort has gone into reaction and spectroscopy studies of these clusters, little effort is visible in quantitative microscopy of these clusters.[8,9]

Earlier microscopy work on osmium carbonyl clusters using high-resolution electron microscopy (HREM) shows particle size measurements based on radius measurements. But the technique fails to be reliable for clusters less than 1 nm in size due to the complications involved with naive interpretation of such images.[10,11] HREM has been used routinely[12] to study ultrasmall catalyst particles. While this technique is especially useful to study shapes, and preferred sites of individual clusters,[13,14] it is important to note that estimated cluster sizes in such images will have an error at least equal to the microscope resolution (∼2 Å). Microscope operating parameters complicate the image information significantly, especially near the resolution limit. Rough and noisy substrates, characteristically used in catalysis, will make image interpretation of these small objects difficult, owing to a highly demanding signal/noise ratio in HREM. Another alternative of microdiffraction has been attempted in a scanning transmission electron microscopy (STEM) of silica-supported $Os_{10}C(CO)_{24}^{-2}$ compound to determine structure of these clusters.[15]

After Crewe et al.[16] first demonstrated the use of STEM to image single atoms with high atomic number such as uranium ($Z = 92$), a variety of papers were written by Lamvik,[17] Wall,[18] Isaacson,[19] and Langmore.[20] These studies employed this technique for mass measurement, particularly in biological materials. They showed the promise offered by "*Z*-contrast microscopy" owing to the strong *Z* dependence of the dark-field image intensity under Rutherford scattering conditions, at high angles (∼40 mrad).

Incoherent electron imaging, one form of *Z*-contrast microscopy, has been used as a powerful technique for imaging single atoms and biological samples. However, the potential of this technique was not recognized fully, in studying supported metal clusters. For imaging of single atoms and linear objects such as DNA molecules studied earlier, effects of electron beam

* Corresponding author.
[⊗] Abstract published in *Advance ACS Abstracts,* April 1, 1996.

0022-3654/96/20100-6385$12.00/0

longitudinal coherence may not be significant. However, for 3-D crystalline objects, sufficient care was not taken until fairly recently,[21,22] to remove these effects. In this research on high-angle (∼96 mrad) annular dark-field (HAADF) images, we suppress this coherence by using high angles of scattering. We studied relative mass quantization on graphite-supported, small organometallic clusters of rhenium ($Z = 75$). From our analysis on 6-Re clusters deposited on graphite, we find a monosize distribution and that these clusters are fairly stable. Similar analysis on 6-, 7-, and 8-Re clusters on graphite shows that the species with 7 and 8 rhenium atoms disintegrate and sinter into various sizes. In our technique, we determine size distribution based on the statistical analysis of electron scattered intensity, which remains conserved independent of the electron-optical parameters.

Experimental Section

Sample preparation is extremely critical and requires uniform, thin, and low-noise supports such as graphite.[23] Graphite flakes were agitated ultrasonically, in ethanol, to yield thin (∼50 Å) films which were then deposited on a 3-mm-diameter holey carbon TEM grid. Three rhenium compounds, namely, $[PPN]_2[H_2Re_6C(CO)_{19}]$, $[PPN]_3[Re_7C(CO)_{21}]$, and $[PPN]_2[Re_8C(CO)_{24}]$,[24] consisting of 6, 7, and 8 Re atoms, were used. Two types of samples were made: 6-Re compound on graphite and 6-, 7-, and 8-Re compounds, in equal proportions, on graphite. The compounds were dissolved in a solvent such as acetone. The solution concentration was $\sim 10^{-4}$ M. Small volumes (∼2 μL) of the solution were deposited on the TEM grid. After the solvent evaporated, the clusters were found to be randomly deposited on the graphite substrate. It is very important to carry out the above procedure in a drybox; under ambient conditions severe aggregation occurred.[25] After deposition, to remove carbonaceous contaminants from the substrate, the samples were baked in a cryopumped annealing furnace at rough vacuum and heated to about 100 °C.

Imaging was performed on a field emission gun (FEG) Vacuum Generators STEM, HB501 operated at 100 kV. The microscope was equipped with digital scanning acquisition software by Gatan's Digiscan. The images were 512 × 512 pixels in size, and each pixel intensity had a precision of 16 bits. For the bright-field (BF) images the collector aperture had an inner half-angle of 2.5 mrad. For the HAADF images, the inner collection half-angle was masked to be 96 mrad. The outer collection half-angle for the annular detector was ∼345 mrad. The focused probe size for the objective aperture used here was ∼3.6 Å.

Image analysis was performed by scanning the high-magnification high-angle annular dark field images with pixel size ∼2.3 Å. These images were first Fourier filtered to remove low-frequency (∼100 Å wavelength) noise coming from the substrate. This helped us manually identify the coordinates of the particles more clearly. Using these locations of the particles in raw unfiltered dark-field images, actual intensity measurements were performed. Automatic detection of particles is difficult, and so we actually used a more conventional manual method such as described by Treacy.[9] The background-subtracted intensities of these brighter pixels were transformed into scattering cross sections and were plotted as a histogram. This image processing and analysis was carried out using Gatan's DigitalMicrograph and special image analysis programs written for the purpose.

The dark-field and bright-field scintillator−photomultiplier detectors were roughly calibrated by using graphite thickness as an internal standard. By measuring the decrease in main-

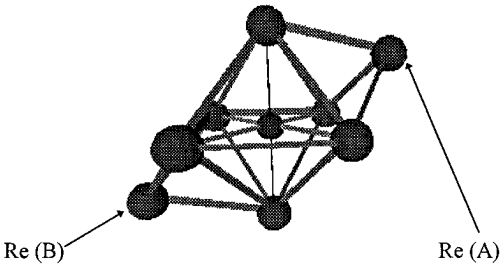

Figure 1. Schematic of rhenium compounds with 6-, 7-, and 8-Re atoms surrounding an internal carbon atom. Re (A) and Re (B) are two capping atoms on the triangular faces of the octahedral compound of 6-Re.

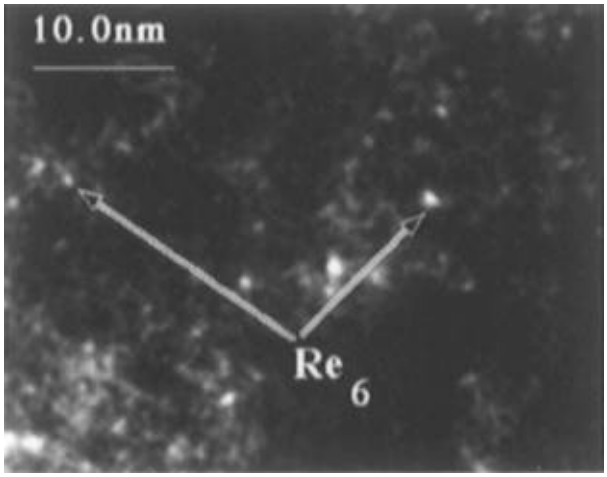

Figure 2. Scanning transmission electron microscope (STEM) annular dark field image of 6-Re atom clusters deposited on graphite.

beam intensity after passing through a certain graphite area in a bright field image, we measured graphite thickness for that area. By calculating the cross section for this graphite thickness and for our dark-field detector configuration, we determined the dark-field efficiency. To have a reasonable calibration, we performed this analysis on several different areas within the same image and on different samples. Although these detectors enhance the weak dark-field signals significantly, their response to both the BF and DF signals can be dissimilar, especially if sufficient care is not taken. A pulse-counting approach in our detectors can provide absolute electron counts (with poorer statistics) and, hopefully, absolute scattering cross sections. However, in the absence of such data, the present calibration routine is fairly reliable for relative mass measurements.

Absolute measurements of the scattering cross section are more difficult to make and are less accurate than the relative measurements between samples which is the emphasis of this paper. Our results presented later show disagreement of a factor of ∼3 between first Born approximation calculations of scattering power by a rhenium atom and our measurements. We discuss this disagreement later and propose methods to measure and calculate cross sections more accurately.

Results and Discussion

Figure 1 presents the schematics of the atomic configuration in clusters of 6-, 7-, and 8-Re atoms surrounding an internal carbon atom.[26] Atoms A and B, when removed, give an octahedrally bonded 6-Re compound; attaching atoms A and B successively, yields 7-Re and 8-Re compounds. Figure 2 shows a high magnification annular dark field (ADF) image of the 6-Re atom species of clusters on a graphite support. The clusters appear as bright speckles against a dark background. Coherent

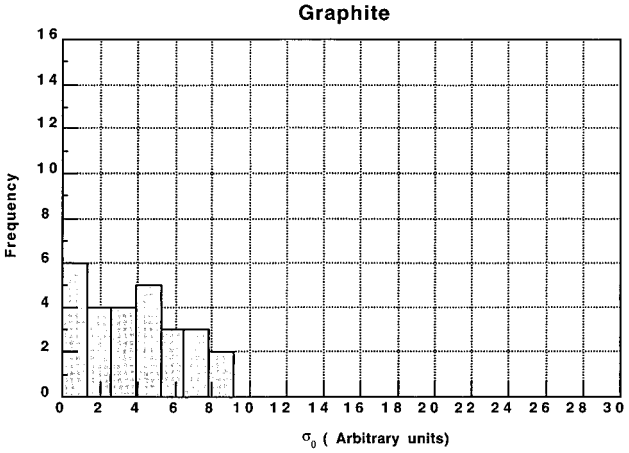

Figure 3. Histogram of intensity from bare graphite imaged at 96 mrad. The contribution from the graphite support to the scattered intensity is very small.

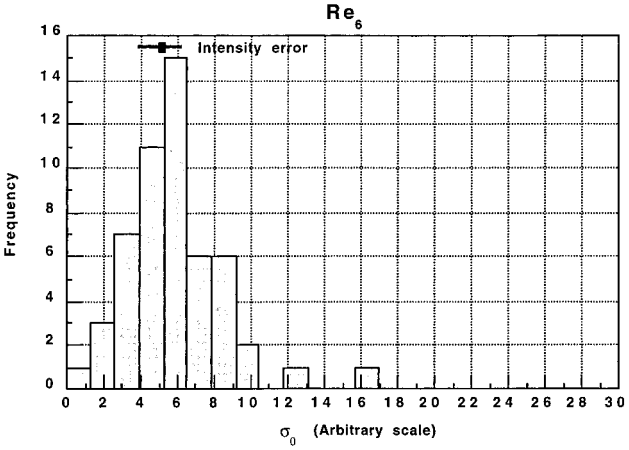

Figure 4. Histogram of intensity from Re_6 particles imaged at 96 mrad. Note a single broad peak near $6\sigma_0$. The contribution from the graphite support to the intensity in the above intensity range is very small (Figure 3).

contributions to the scattered intensity from these clusters can be calculated. These contributions at lower scattering angles (∼40 mrad) can be very large for certain cluster orientations. Also, the intensity from substrates gives rise to speckle contrast, which could also be large and may not be eliminated until one uses sufficiently high angles of scattering (∼96 mrad). Since the cluster/support interactions are unknown, we rely on using high angles of scattering to remove the coherent contributions and the speckle from the dark-field image intensity.

Figure 4 is an intensity histogram obtained after analyzing samples with 6-Re clusters deposited on graphite supports. It shows a single, broad peak showing a monosize dispersion, which we believe has a mean size of 6-Re atoms ($6\sigma_0 \sim 0.048$ Å^2). The ordinate gives the number of these particles. Similar analysis, on the 6-, 7-, and 8-Re atom clusters deposited on graphite, does not show three distinct peaks corresponding 6-, 7-, and 8-Re atoms (Figure 5). Instead, one notices the first peak being very pronounced, and, within intensity measurement error, which is ±20%, it is equivalent to the peak of 6-rhenium atoms in Figure 4. Following this peak, one may note the extended size distribution. This indicates that 7- and/or 8-Re clusters are fragmenting to give 6-Re clusters, possibly due to exposure to the high-energy electron beam, and then sintering into various sizes. The sintered particles have a maximum size of ∼20 atoms. These observations are consistent with similar measurements on a sample of only 8-Re clusters deposited on graphite. On 8-Re, like in Figure 5, we find a sharp peak

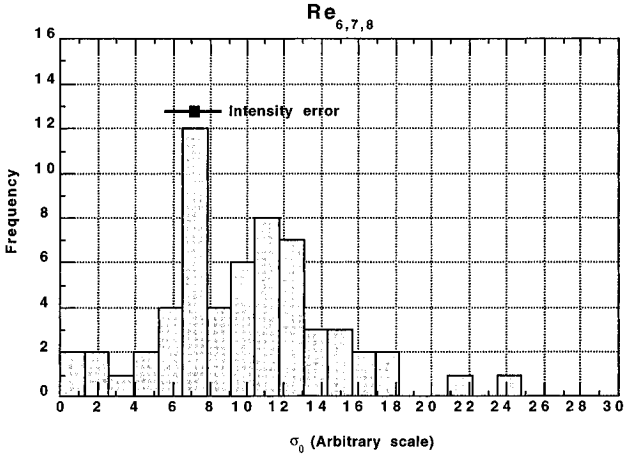

Figure 5. Intensity histogram from Re_6, Re_7, and Re_8 particles on graphite, imaged at 96 mrad. Note the large size variation along the *x* axis. The first peak is believed to be due to Re_6 clusters and is particularly pronounced. These Re_6 clusters were possibly formed after the 7- and the 8-Re clusters decomposed upon electron irradiation. The contribution from the graphite support to the above intensity range is very small (Figure 3).

TABLE 1: Theoretical Scattering Cross Sections from 6-, 7-, and 8-Re Atom Clusters

	6-Re atoms	7-Re atoms	8-Re atoms
σ (Å^2)	0.162	0.189	0.216

followed by a distribution of sizes. This peak results, most likely, from the previously known stable 6-Re clusters formed after fragmentation of 8-Re clusters. These unstable 8-Re clusters exhibit sintering into varying sizes up to a maximum of 12-Re atoms. Intensity analysis on bare graphite does not exhibit many counts in these higher intensity regimes (Figure 3). Analysis on bare graphite was performed only on areas higher than average such as surface steps and heavy contaminant atoms on graphite. Figure 3 shows that the intensity contribution even from these areas on the substrate is significantly smaller than that arising from the monodisperse particles on graphite. Under naive interpretation, these areas could be perceived as metal particles.

The 6-Re atom clusters show a clear monosize distribution, which we suppose to be six atoms based on the high stability imparted by the structure. Absolute measurements, which have proven difficult so far, disagree with absolute cross sections by a factor of ∼3. On the same intensity scale, within an error of ±20%, a sample of 6-, 7-, and 8-Re shows a range of sizes, while a sample with 6-Re shows a single peak. In both cases the first peak is positioned near 0.048 Å^2. We define this value as $6\sigma_0$ to represent 6 times the measured cross section of one rhenium atom. Accordingly, we transform our intensity scales on the histograms (Figures 3−5) in terms of σ_0. The first peak position shows a systematic matching for different samples with 6-Re and 6-, 7-, and 8-Re on graphite. Therefore, our assumption of this peak corresponding to 6-Re is reasonable. Theoretical calculations of cross sections of these clusters are given in Table 1 and are based on convolution of the objective aperture over the sample and multiplication with the integrated differential scattering cross section over the angular range of the annular dark-field detector (96−345 mrad). Calculations of the electron scattering factor were based on the first Born approximation, and analytical expressions for the X-ray scattering factor in the range of electron scattering vector used.[27] More exact partial-wave method calculations yield a theoretical scattering cross section ∼30% lower than those expected by using a first Born approximation and is in better agreement than

with the first Born approximation.. The discrepancy between theoretical and measured cross sections is consistent for different samples and may be a result of systematic errors, detector calibration being most important among them.

In cases where these clusters are strongly attached to supports such as γ-Al_2O_3, by infrared spectroscopy it has been found that the 6-Re clusters are quite stable, while the 8-Re clusters disintegrate.[28] This follows from the bonding of rhenium atoms with an internally caged C atom within these clusters. The 6-Re atoms from an octahedral configuration and bond very strongly to the interior carbon atom (Figure 1). In an 8-Re cluster, however, there also exist two *capping* Re atoms not bonded as strongly to the carbon atom. Therefore, one would exist two two atoms in 8-Re clusters to break apart easily and form 6-Re and two Re atoms. In Figure 5, we notice that graphite-supported 6-, 7-, and 8-Re clusters exhibit a pronounced peak corresponding to 6-Re and a range of different sizes. We believe that these clusters, weakly bonded to a substrate like graphite, disintegrate as they do on other substrates. However, they also sinter into several different sizes. Since the height of the first peak is not in proportion to the volumes of all the three cluster species, it it possible that many of the fragmented clusters sintered together into a range of larger sizes. The fragmentation of 7- and/or 8-Re clusters was, most likely, enhanced by the high-energy electron probe. Reduction fragmentation of these clusters has also been observed in solution studies.[24] However, it is difficult to separate the inherent chemical character of these clusters from the possible beam-induced damage. In any event, there is a good agreement between our microscopy results on graphite-supported clusters and infrared spectroscopy results from alumina-supported clusters.

Calculations show that the image intensity contributions from the ligands are less than 5% of the metal atoms. Furthermore, these ligands were possibly removed by the high-energy electron beam. In any case, their contribution to the scattered intensity was ignored.

Since one notices that the experimental cross sections are lower than the theoretical numbers by a factor of ∼3, one may speculate that the six-rhenium particles, like the seven and eight-rhenium compounds, are possibly fragmenting. The measured cross sections are close to doublets of rhenium atoms. However, we believe that this may not be true owing to the following reasons: (1) The clusters in the image appear too large to be single or double atoms of rhenium. (2) The scattered intensity from the clusters was possibly leaked into the neighboring pixels in the image and was subtracted as a part of the background. (3) There may be an error in our measurements of the dark-field detector efficiency. By using a pulse-counting approach, this can be improved. (4) The clusters may have possibly moved during the time of image acquisition. However, this appears inconsistent with the observed long-term stability of the clusters.

Conclusion

Using high-angle dark-field imaging in STEM, we have made approximate mass measurement on supported organometallic clusters with 6-, 7-, and 8-Re atoms. Using our technique, we demonstrate that the 6-Re atom clusters exhibit high resistance to fragmentation unlike the seven and 8-Re atom clusters; disintegration was possibly caused by a high-energy electron beam probe. Seven- and eight-rhenium compounds tend to fragment and resinter into various sizes up to ∼20 atoms. We believe that the larger clusters, i.e., 7- and 8-Re clusters, fragment to give stable 6-Re clusters and the capping atoms; sintering into larger sizes follows. In this work, we are able to show the potential of the *Z*-contrast technique as applied to mass measurement of ultra-small particles, in particular, organometallics. Details on theory of the technique will be published elsewhere.

Acknowledgment. The research at University of Illinois was supported by grants from National Science Foundation, No. NSF-DMR89-20538 and from Department of Energy, No. DEFG02-91ER45439. Thanks are also due to AT&T Bell Laboratories for kindly donating the STEM to the Frederick Seitz Materials Research Laboratory, University of Illinois at Urbana−Champaign.

References and Notes

(1) Golden, J. H.; et al. *Science* **1995**, *268*, 1463−1466.
(2) Reetz, M. T.; et al. *Science* **1995**, *267*, 367.
(3) Hagfelt, A.; Gratzel, M. *Chem. Rev.* **1995**, *95*, 49.
(4) Parkyns, N. D. *Proc. Int. Congr. Catal. 3rd 1964*, **1965**, *2*, 914.
(5) Cox, D. M.; Kaldor, A.; Fayet, A.; et al. *ACS Symp. Ser.* **1990**, *437*, 172−187.
(6) Lyding, J. W.; et al. *J. Vac. Sci. Technol. A* **1988**, *6*, 363−367.
(7) Poppa, H. *Catal. Rev. Sci. Eng.* **1993**, *35*, 359−398.
(8) Gallezot, P.; Richard, D.; Bergeret, G. *ACS Symp. Ser.* **1990**, *437*, 150−159.
(9) Treacy, M. M. J.; Rice, S. B. *J. Microsc.* **1989**, *156*, 211−234.
(10) Flynn, P. C.; Wanke, S. E.; Turner, P. S. *J. Catal.* **1974**, *33*, 233−248.
(11) Treacy, M. M. J.; Howie, A. *J. Catal.* **1980**, *63*, 265−269.
(12) Schwank, J.; Allard, L. F.; Deeba, M.; Gates, B. C. *J. Catal.* **1983**, *84*, 27−37.
(13) Iijima, S.; Ichikawa, M. *J. Catal.* **1985**, *94*, 313−318.
(14) Yao, M.-H.; Smith, D. J.; Kalakkad, D.; Datye, A. K. *Suppl. Z. Phys. D* **1993**, *26*, S79−81.
(15) Mochel, M. E.; et al. *Proc 44th Annu. Meeting Electron Microsc. Soc. Am.* **1986**, 696−697.
(16) Crewe, A. V.; Wall, J. S. *Science* **1970**, *168*, 1338−1340.
(17) Lamvik, M. K. *J. Mol. Biol.* **1978**, *122*, 55−68.
(18) Wall, J. S. *ITRI/SEM* **1979**, *2*, 291−303.
(19) Isaacson, M.; Kopf, D.; Ohtsuki, M.; Utlaut, M. *Ultramicroscopy* **1979**, *4*, 101−104.
(20) Langmore, J. P.; Wall, J. S.; Isaacson, M. S. *Optik* **1973**, *38*, 335−350.
(21) Jesson, D. E.; Pennycook, S. J. *Proc. R. Soc. London A* **1993**, *441*, 261−281.
(22) Treacy, M. M. J.; Gibson, J. M. *Ultramicroscopy* **1993**, *52*, 31−53.
(23) Johansen, B. V. *Micron* **1974**, *5*, 209.
(24) Hayward, C. M. T.; Shapley, J. R. *Organometallics* **1988**, *7*, 448−452.
(25) Devenish, R. W.; Mulley, S.; Heaton, B. T.; Longoni, G. *J. Mater. Res.* **1992**, *7*, 2810−2816.
(26) Ciani, G.; et al. *J. Organomet. Chem.* **1983**, *244*, C27 and references therein.
(27) Ibers, J. A.; Hamilton, W. C. *Int. Tables for X-ray Crystallography*; Kynoch Press: Birmingham, UK, 1973; Vol. IV, p 99.
(28) Lane, P. D. Ph.D. Thesis, University of Illinois at Urbana−Champaign, 1995.

JP953718N